**Cell Chemical Biology, Volume *23***

## Supplemental Information

# An RNA-Based Fluorescent Biosensor for High-Throughput Analysis of the cGAS-cGAMP-STING Pathway

**Debojit Bose, Yichi Su, Assaf Marcus, David H. Raulet, and Ming C. Hammond**

**Supplemental Information**

**for**

# An RNA-based fluorescent biosensor for high-throughput analysis of the cGAS-cGAMP-STING pathway

Debojit Bose*, Yichi Su*, Assaf Marcus,
David Raulet, Ming C. Hammond

*These authors contributed equally to the work

**Table of contents**

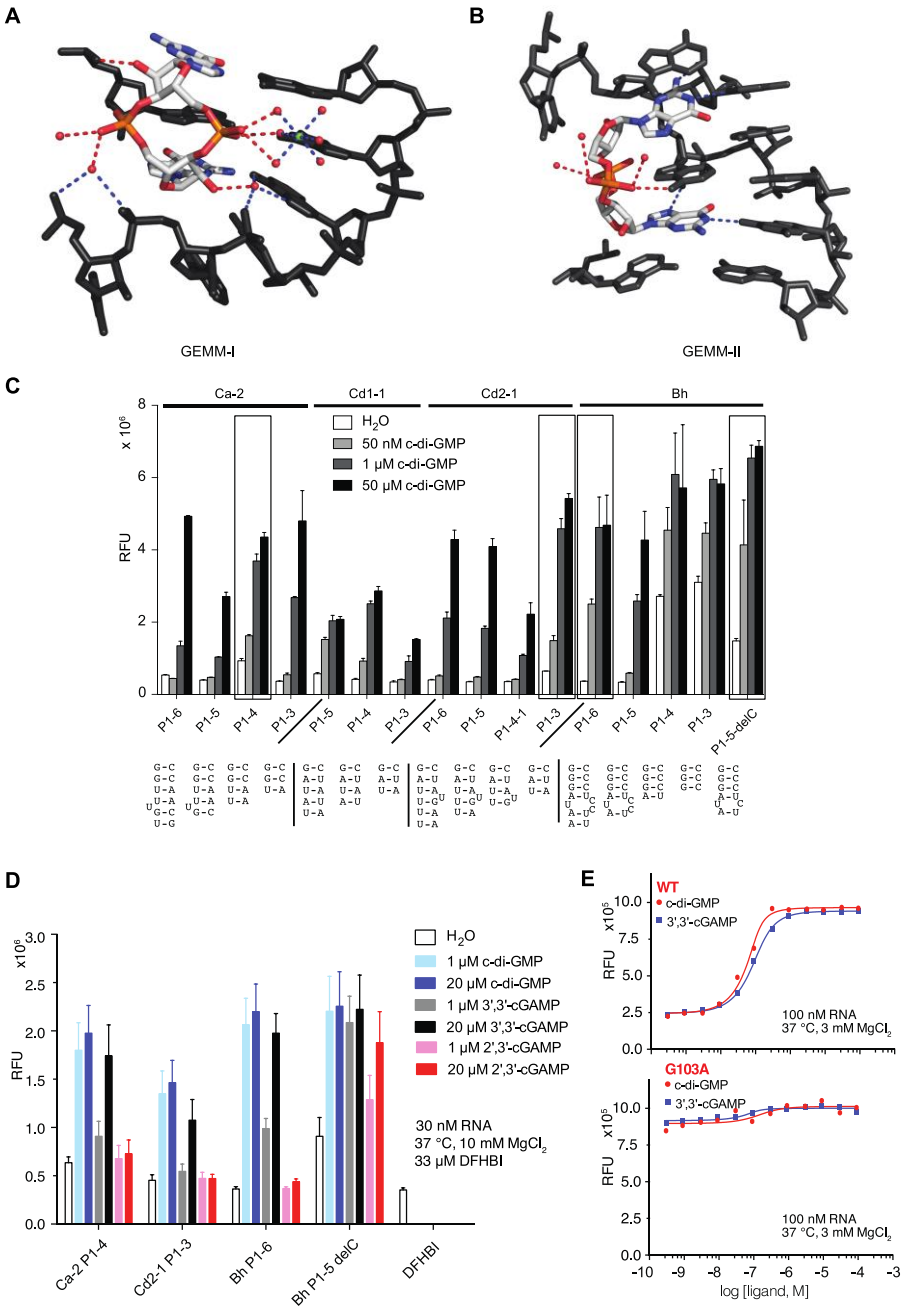


**Figure S1 (related to Figure 1). Screen and mutagenesis analysis for GEMM-II riboswitch-based 2′, 3′-cGAMP biosensors.**

Interactions between (A) GEMM-I riboswitch (PDB code 3MXH) or (B) GEMM-II riboswitch (PDB code 3Q3Z) with 2′-hydroxyls and phosphodiester oxygens of c-di-GMP. The interactions are shown in red dashes. (C) Screening of different phylogenetic and stem varients of GEMM-II riboswitch for developing 2′, 3′-cGAMP biosensor. Error-bars represent the standard deviation of 3 independent replicates. (D) Analysis of biosensor hits from screening in (C) for their response to different cylic dinucloetides. (E) Selectivity profiles of Bh P1-5 delC WT and G103A biosensors, *in vitro* fluorescence activation and binding affinity measurements for Bh P1-5 delC variants with bacterial cyclic dinucleotides, c-di-GMP and 3′,3′-cGAMP. Error bars indicate standard deviations for three independent replicates.

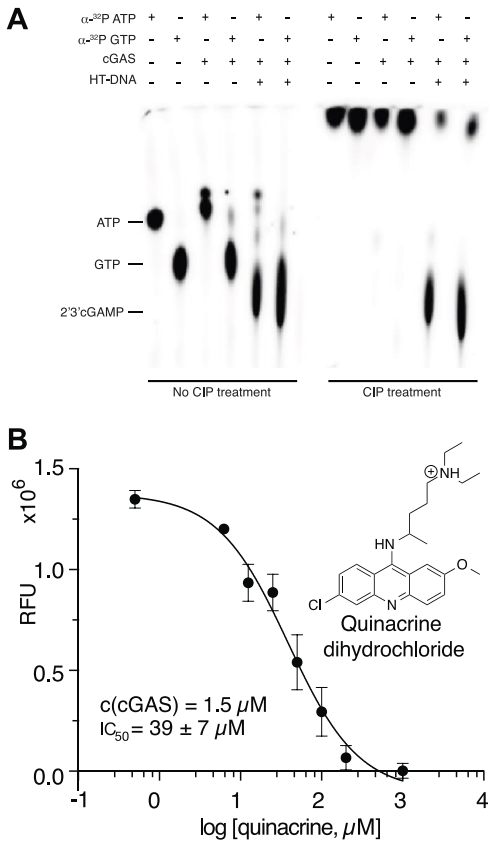


**Figure S2 (related to Figure 2, Figure 3). TLC-based cGAS activity assay and RNA biosensor-based cGAS inhibition assay.**
(A) TLC-based assay with radiolabeled substrates to assess cGAS activity. Calf intestinal alkaline phosphatase (CIP) was used to remove free nucleotide triphosphate. Image is representative of multiple independent experiments. (B) Initial analysis of cGAS inhibition by quinacrine (QC) via RNA-based fluorescent biosensor. The determined $IC_{50}$ was later revealed to be artefactual due to the intercalating effect of QC to the RNA-based biosensor. Error bars indicate standard deviations for three independent replicates.

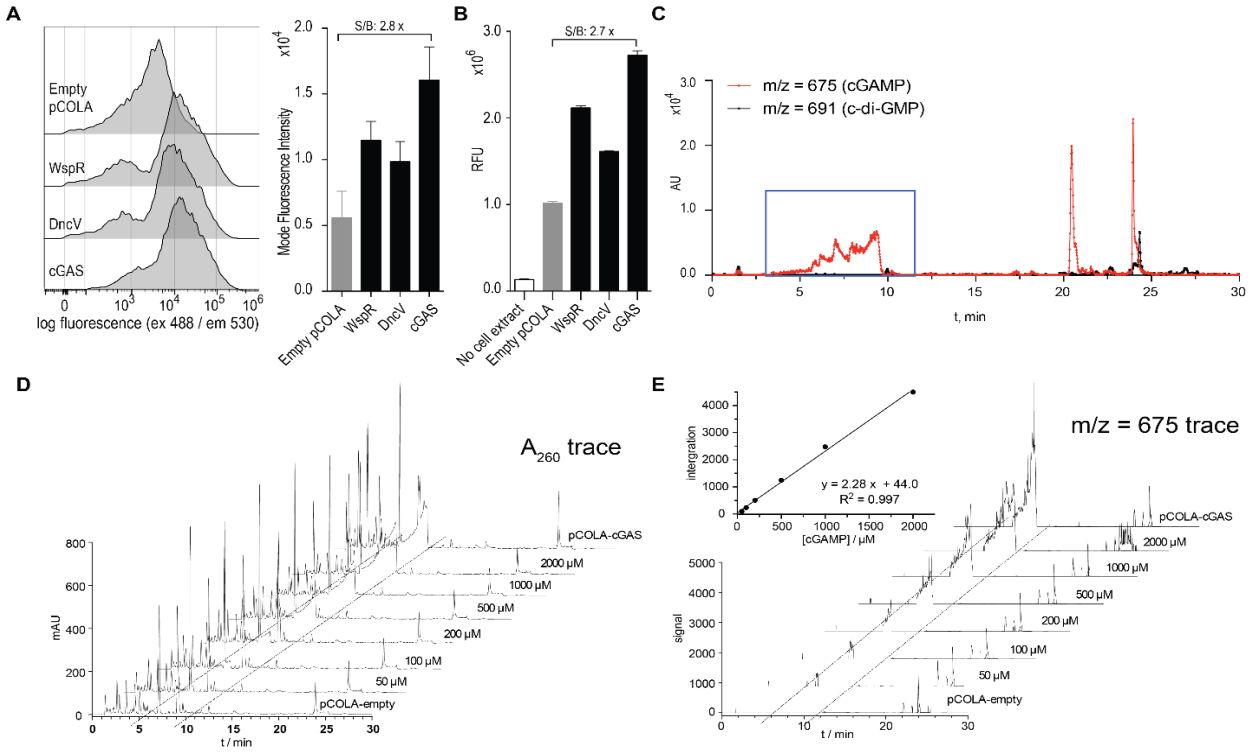


**Figure S3 (related to Figure 4). Application of fluorescent biosensor to detect 3',3'-cGAMP and other cyclic dinucleotides in bacterial cells expressing synthase enzymes.**
(A) Representative flow cytometry analysis of live *E. coli* expressing plasmids encoding both biosensor and cyclic dinucleotide synthases after incubation in media containing DFHBI-1T. Fluorescence values on x-axis are shown using HyperLog scaling. The average mode fluorescence intensity (MFI) from two independent biological replicates are shown in the bar graph, error bars depict standard deviations. (B) *In vitro* fluorescence biosensor-based analysis of cyclic dinucleotide content of cell extracts from *E. coli* expressing the corresponding cyclic dinucleotide synthases. Error bars depict standard deviations for two independent biological replicates. (C) LC-MS analysis of cell extract from *E. coli* expressing a plasmid encoding cGAS. Mass trace corresponding to 2′,3′-cGAMP (m/z = 675, red) and c-di-GMP (m/z = 691, blue) were shown. Signal peaks corresponding to 2′,3′-cGAMP production were boxed. (D, E) Quantitation of 2′, 3′-cGAMP in *E. coli* expressing a plasmid encoding cGAS. Cell extracts from *E. coli* expressing an empty pCOLA vector plasmid was added with varied concentrations of 2′, 3′-cGAMP and then assayed by LC-MS, with 260 nm absorbance (D) and mass spec signal (E) shown. Standard curve for quantifying 2′, 3′-cGAMP based on the integration of mass spec signal was shown in inset in (E). All the data were collected on an Agilent 1260 Infinity LC-MS system equipped with a Poroshell 120 C-18 column. Error bars indicate standard deviations for three independent replicates.

**Measuring activity of expressed cGAS in live bacterial cells**
Prior work in our lab has established riboswitch-based biosensors for metabolite detection in live *E. coli* (Hallberg et al., 2016; Kellenberger et al., 2015a; Kellenberger et al., 2015c; Kellenberger et al., 2013; Su et al., 2016), so we were interested to benchmark the performance of the 2′, 3′-cGAMP biosensor under similar *in vivo* conditions. In order to test this, we inserted the biosensor construct into the tRNA scaffold (Kellenberger et al., 2015b; Ponchon and Dardel, 2007), then co-expressed the fluorescent biosensor along with empty vector or enzymes that synthesize different cyclic dinucleotides in *E. coli* BL21-Star cells. WspR from *Pseudomonas fluorescens* produces c-di-GMP, DncV from *Vibrio cholerae* produces 3′, 3′-cGAMP, and cGAS from *Homo sapiens* produces 2′, 3′-cGAMP. After incubating cells with the profluorescent dye DFHBI-1T (Song et al., 2014), the cellular fluorescence was analyzed by flow cytometry, which provides high-throughput, single-cell quantitation of metabolites as detected by the fluorescent biosensor. The heterogeneity observed in the fluorescence values for a cell population is attributed to differences in multiple factors in the experiment, such as plasmid copy number, enzyme expression level, RNA biosensor expression level, and cell size in live, replicating *E. coli*. To address this issue, the mode fluorescence intensity (MFI, defined as the value with

the most observations) of each population was analyzed since this value was consistent between independent biological replicates.

As expected, significant fluorescence activation was observed upon co-expression of each enzyme (Fig. S3A), because the Bh P1-6 G103A biosensor is capable of binding 3′, 3′-cGAMP, c-di-GMP, and 2′, 3′-cGAMP (listed in order of affinity). However, the degree of fluorescence activation did not correspond to the relative affinity of the biosensors for the different cyclic dinucleotides. Instead, it appears to correlate directly to the amount of each cyclic dinucleotide produced by the enzymes *in vivo*, as the identical trend was observed when we performed an aqueous-organic extraction of cell lysates and analyzed the extracts containing cyclic dinucleotides using the biosensor (Fig. S3B). Notably, given that the biosensor has poorer affinity for 2′, 3′-cGAMP versus the two 3′, 3′-linked cyclic dinucleotides, this result implies that cGAS is highly activated by binding to endogenous genomic DNA to produce an extremely large amount of 2′, 3′-cGAMP in *E. coli*. In addition, there is likely no endogenous phosphodiesterase capable of efficiently hydrolyzing the compound. Accordingly, LCMS analysis showed that 2′, 3′-cGAMP is highly abundant in the cell extracts, building up to ~0.5 mM concentration based on our standard curve (Fig. S3C, D, E). It should also be noted that *E. coli* has endogenous c-di-GMP (Weber et al., 2006), so basal activation is observed for cells harboring the empty pCOLA vector, both in vivo and in extracts. Thus, the fluorescence activation of the biosensor we observed is likely lower than the theoretical maximum fold activation if we compared to cells that have no c-di-GMP. For example, to our knowledge mammalian cells do not produce c-di-GMP, except for those engineered for synthetic biology applications (Folcher et al., 2014). In all, these live-cell flow cytometry results demonstrate that our first-generation biosensors are capable of detecting 2′,3′-cGAMP in the complex setting of bacterial cells, which lays the foundation for achieving 2′,3′-cGAMP detection in live mammalian cells.

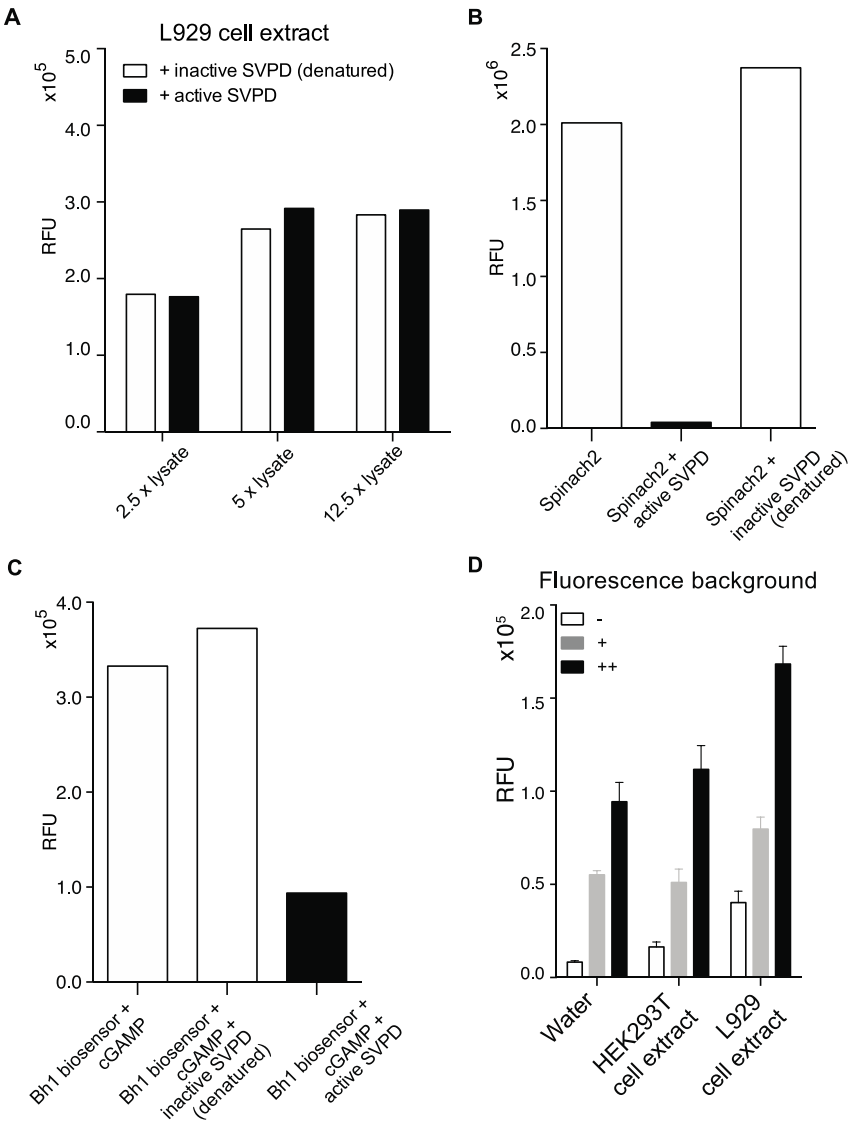


**Figure S4 (related to Figure 4). Source of fluorescence background in biosensor-based analysis of mammalian cell extracts.**

(A-C) SVPD degradation experiments to rule out basal 2′, 3′-cGAMP in L929 cells. (A) Fluorescence readings for varied concentration of mock-transfected L929 cell extracts treated with active or denatured SVPD prior to biosensor addition. (B) Fluorescence readings for Spinach2 aptamer treated with active or denatured SVPD. (C) Fluorescence readings for 2′,3′-cGAMP treated with active or denatured SVPD prior to biosensor addition. (D) The origin of background fluorescence in mock-stimulated cell extract was investigated. (-, cell extract alone; +, cell extract + DFHBI; ++, cell extract + biosensor + DFHBI.) Error bars indicate standard deviations for three independent biological replicates.

**Table S1 (related to Figure 1).** GEMM-II riboswitch-based biosensors sequences

| Name | Sequences |
|---|---|
| Ca-2 P1-6 | GATGTAACTGAATGAAATGGTGAAGGACGGGTCCA***TGTTTGG***AAACAATGAT GAATTTCTTTAAATTGGGCACTTGAGAAATTTTGAGTTAGTAGTGCAACCGA***C CAACG***TTGTTGAGTAGAGTGTGAGCTCCGTAACTAGTTACATC |
| Ca-2 P1-5 | GATGTAACTGAATGAAATGGTGAAGGACGGGTCCA***GTTTGG***AAACAATGATG AATTTCTTTAAATTGGGCACTTGAGAAATTTTGAGTTAGTAGTGCAACCGA***CC AAC***TTGTTGAGTAGAGTGTGAGCTCCGTAACTAGTTACATC |
| Ca-2 P1-4 | GATGTAACTGAATGAAATGGTGAAGGACGGGTCCA***TTGG***AAACAATGATGAA TTTCTTTAAATTGGGCACTTGAGAAATTTTGAGTTAGTAGTGCAACCGA***CCAA*** TTGTTGAGTAGAGTGTGAGCTCCGTAACTAGTTACATC |
| Ca-2 P1-3 | GATGTAACTGAATGAAATGGTGAAGGACGGGTCCA***TGG***AAACAATGATGAAT TTCTTTAAATTGGGCACTTGAGAAATTTTGAGTTAGTAGTGCAACCGA***CCA***TT GTTGAGTAGAGTGTGAGCTCCGTAACTAGTTACATC |
| Cd1-1 P1-5 | GATGTAACTGAATGAAATGGTGAAGGACGGGTCCA***TATAG***AAACTGTGAAGT ATATCTTAAACCTGGGCACTTAAAAGATATATGGAGTTAGTAGTGCAACCTG***C TATA***TTGTTGAGTAGAGTGTGAGCTCCGTAACTAGTTACATC |
| Cd1-1 P1-4 | GATGTAACTGAATGAAATGGTGAAGGACGGGTCCA***ATAG***AAACTGTGAAGTA TATCTTAAACCTGGGCACTTAAAAGATATATGGAGTTAGTAGTGCAACCTG***CT AT***TTGTTGAGTAGAGTGTGAGCTCCGTAACTAGTTACATC |
| Cd1-1 P1-3 | GATGTAACTGAATGAAATGGTGAAGGACGGGTCCA***TAG***AAACTGTGAAGTAT ATCTTAAACCTGGGCACTTAAAAGATATATGGAGTTAGTAGTGCAACCTG***CT A***TTGTTGAGTAGAGTGTGAGCTCCGTAACTAGTTACATC |
| Cd2-1 P1-6 | GATGTAACTGAATGAAATGGTGAAGGACGGGTCCA***TTTTAG***AAACTGAGAAG TATATCTTATTATTGGGCATCTGGAGATATATGGAGTTAGTGGTGCAACCGG ***CTATGAA***TTGTTGAGTAGAGTGTGAGCTCCGTAACTAGTTACATC |
| Cd2-1 P1-5 | GATGTAACTGAATGAAATGGTGAAGGACGGGTCCA***TTTAG***AAACTGAGAAGT ATATCTTATTATTGGGCATCTGGAGATATATGGAGTTAGTGGTGCAACCGG***C TATGA***TTGTTGAGTAGAGTGTGAGCTCCGTAACTAGTTACATC |
| Cd2-1 P1-4 | GATGTAACTGAATGAAATGGTGAAGGACGGGTCC***TTAG***AAACTGAGAAGTAT ATCTTATTATTGGGCATCTGGAGATATATGGAGTTAGTGGTGCAACCGG***CTA TG***TTGTTGAGTAGAGTGTGAGCTCCGTAACTAGTTACATC |
| Cd2-1 P1-3 | GATGTAACTGAATGAAATGGTGAAGGACGGGTCC***TAG***AAACTGAGAAGTATA TCTTATTATTGGGCATCTGGAGATATATGGAGTTAGTGGTGCAACCGG***CTA***T TGTTGAGTAGAGTGTGAGCTCCGTAACTAGTTACATC |
| Bh P1-6 | GATGTAACTGAATGAAATGGTGAAGGACGGGTCC***AATAGGG***AAGCAACGAA GCATAGCCTTTATATGGACACTTGGGTTATGTGGAGCTACTAGTGTAACCGG ***CCCTCCTT***TTGTTGAGTAGAGTGTGAGCTCCGTAACTAGTTACATC |
| Bh P1-5 | GATGTAACTGAATGAAATGGTGAAGGACGGGTCC***ATAGGG***AAGCAACGAAG CATAGCCTTTATATGGACACTTGGGTTATGTGGAGCTACTAGTGTAACCGG***C CCTCCT***TTGTTGAGTAGAGTGTGAGCTCCGTAACTAGTTACATC |
| Bh P1-4 | GATGTAACTGAATGAAATGGTGAAGGACGGGTCC***AGGG***AAGCAACGAAGCA TAGCCTTTATATGGACACTTGGGTTATGTGGAGCTACTAGTGTAACCGG***CCC T***TTGTTGAGTAGAGTGTGAGCTCCGTAACTAGTTACATC |
| Bh P1-3 | GATGTAACTGAATGAAATGGTGAAGGACGGGTCC***GGG***AAGCAACGAAGCAT AGCCTTTATATGGACACTTGGGTTATGTGGAGCTACTAGTGTAACCGG***CCC***T TGTTGAGTAGAGTGTGAGCTCCGTAACTAGTTACATC |
| Bh P1-5 delC | GATGTAACTGAATGAAATGGTGAAGGACGGGTCC***ATAGGG***AAGCAACGAAG CATAGCCTTTATATGGACACTTGGGTTATGTGGAGCTACTAGTGTAACCGG***C CCTCT***TTGTTGAGTAGAGTGTGAGCTCCGTAACTAGTTACATC |

Ca: Bacteria Firmicutes Clostridia Clostridiales Clostridiaceae *Clostridium acetobutylicum* ATCC 824
Cd1: Bacteria Firmicutes Clostridia Clostridiales Clostridiaceae *Clostridium difficile* 630
Cd2: Bacteria Firmicutes Clostridia Clostridiales Clostridiaceae *Clostridium difficile* QCD- 32g58
Bh: Bacteria Firmicutes Bacillales Bacillaceae *Bacillus halodurans* C-125

**Table S2 (related to Figure 1).** GEMM-II biosensor binding affinities and fluorescent turn-on properties

| | Bh P1-5delC | | Bh P1-6 WT | | Bh P1-6 G103A | |
|---|---|---|---|---|---|---|
| | Kd (μM) | Fold turn-on (S/B ratio) | Kd (μM) | Fold turn-on (S/B ratio) | Kd (μM) | Fold turn-on (S/B ratio) |
| c-di-GMP[b] | 0.021 ± 0.008 | - | 0.056 ± 0.012 | 13.1x | >7 | 8.2x |
| 3′, 3′-cGAMP[b] | - | - | >11 | 10.8x | 0.8 ± 0.1 | 9.6x |
| 2′, 3′-cGAMP[a] | 13.4 ± 0.9 | 5.1x | - | - | >65 | 10.3x |

[a]Fold turn-on (or signal-to-background ratio) measured with 200 nM RNA, 100 μM ligand in a 384-well plate
[b]Fold turn-on (or signal-to-background ratio) measured with 100 nM RNA, 100 μM ligand in a 384-well plate

**Supplemental Experimental Procedures**

**Analysis of biosensor binding affinities**

To measure the apparent binding affinities of 2′, 3′-cGAMP biosensors, fluorescence assays were performed with the following conditions: 37 °C, 3 mM $MgCl_2$, 200 nM RNA, and 10 μM DFHBI. The 2′, 3′-cGAMP concentration ($c_{cGAMP}$) was varied, and the fluorescence of the sample with DFHBI but no RNA was subtracted as background to determine relative fluorescence units (RFU). The ratio between the fraction of biosensor that is bound by 2′, 3′-cGAMP and the total 2′, 3′-cGAMP biosensor concentration is given as:

$$ratio\ bound = \frac{[RNA \cdot cGAMP \cdot DFHBI]}{c_{total\ RNA}} = \frac{F - F_{\min}}{F_{\max} - F_{\min}}$$

Thus, for each concentration of 2′, 3′-cGAMP, the fluorescence of its corresponding sample should be:

$$F = \frac{[RNA \cdot cGAMP \cdot DFHBI]}{c_{total\ RNA}} \times (F_{\max} - F_{\min}) + F_{\min}$$

where $F_{min}$ is the fluorescence of the sample containing no 2′, 3′-cGAMP, while $F_{max}$ is the fluorescence of the sample containing highest concentration of 2′, 3′-cGAMP (100 μM).

The apparent dissociation constants $K_d$ were determined by least squares fitting to the following equation in Graphpad Prism software:

$$F = \frac{[RNA \cdot cGAMP \cdot DFHBI]}{c_{total\ RNA}} \times (F_{\max} - F_{\min}) + F_{\min} =$$
$$\left[\frac{c_{total\ RNA} + K_d + c_{cGAMP} - \sqrt{(c_{total\ RNA} + K_d + c_{cGAMP})^2 - 4 \times c_{total\ RNA} \times c_{cGAMP}}}{2 \times c_{total\ RNA}}\right] \times (F_{\max} - F_{\min}) + F_{\min}$$

**Determination of 2′, 3′-cGAMP concentration in *E. coli* cells overexpressing cGAS**

*E. coli* harboring either empty pCOLA vector or pCOLA containing cGAS, DncV, or WspR genes were induced with 1 mM IPTG for 4 h at 37 ºC in 3 mL LB media, then the cells were pelleted and dry weight was measured (0.68, 0.75, 0.53, and 0.62 g, respectively). Cyclic dinucleotides were extracted as described previously (Spangler et al., 2010), with the following modifications. Pelleted cells were frozen at -80 ºC overnight. Frozen cell pellets were thawed and resuspended in 1.4 mL extraction buffer (40% acetonitrile, 40% methanol and 20% $ddH_2O$). Resuspended cells were incubated at room temperature with mild agitation for 20 min. After centrifugation for 5 min at 13,200 rpm, the supernatant was carefully removed and stored on ice. The remaining pellet was extracted twice more as described, with 700 μL extraction solvent each time. The combined supernatants were evaporated to dryness by rotary evaporation and the dried material was resuspended in 300 μL $ddH_2O$. The extract was filtered through a 3 kDa MW cutoff Amicon Ultra-4 Protein Concentrator (Millipore) and used immediately or stored at -20 °C. To obtain a standard curve for quantifying 2′,3′-cGAMP, known concentrations of commercial 2′,3′-cGAMP were doped into extracts from cells expressing empty pCOLA to a final volume of 20 μL. The samples were analyzed by LC-MS and the 675 m/z ion traces (corresponding to 2′,3′-cGAMP) were determined. See SI for details on calculation.

To initiate the fluorescent biosensor reaction, 3 μL of the bacterial cell extract was added to 27 μL of biosensor assay solution containing renatured RNA, DFHBI-1T, and biosensor binding buffer. Final concentrations are 200 nM RNA, 25 μM DFHBI-1T, 40 mM HEPES, pH 7.5, 125 mM KCl, and 10 mM $MgCl_2$. Fluorescence measurements were conducted as described above.

***In vivo* fluorescence assays by flow cytometry**

Preparation of cell samples for flow cytometry was carried out by inoculating 3 mL of LB media (containing carbenicillin and kanamycin) with 150 μL of an overnight culture of BL21 star cells harboring both a pET31b plasmid encoding RNA-based biosensor and a pCOLA plasmid encoding cyclic-di-nucleotide synthetase. Cells were grown aerobically to an $OD_{600}$ ~ 0.3 - 0.5, then induced with 1 mM IPTG at 37 °C for 4 hrs. Cell density was measured by $OD_{600}$, and diluted in PBS media containing 100 μM DFHBI-1T to a concentration that gives a flow cytometer analysis rate of around 1000 - 2000 events per second. Cellular fluorescence was measured for 30,000 cells using an Attune NxT Acoustic Focusing Cytometer (Life Technologies).

**Determination of 2′, 3′-cGAMP concentration in *E. coli* cells overexpressing cGAS**

From the linear regression of the standard curve, shown in Figure S3, fitting the standard curve to equation $Y = mX + C$ gave $Y = 2.49X - 7.46$ with an $R^2$ value of 0.99.

The dry weight of the cGAS expressing cell pallet was 0.75 g. This was lysed, extracted and concentrated to give 250 µL cell extract, and 20 µL of the cell extract was loaded in LC-MS.

Thus, the concentration of 2′,3′-cGAMP in the 20 µL measurement solution was calculated to be:

$$c\ (cGAMP) = \frac{Y - C}{m} = \frac{3372 + 7.46}{2.49 \times 1000}\ mM = 1.36\ mM$$

The amount of 2′,3′-cGAMP in the 250 µL cell extract was:

$$n(cGAMP) = c(cGAMP) \times volume = 1.36\ mM \times 250\ \mu L = 0.34\ \mu mol$$

The dry weight of single E. coli cell is $10^{-12}$ g, which gives:

$$number\ of\ cells = \frac{cell\ pallet\ weight}{dry\ weight\ of\ single\ cell} = \frac{0.75}{10^{-12}} \approx 0.75 \times 10^{12}$$

The amount of 2,3-cGAMP per cell was determined to be:

$$n(cGAMP\ per\ cell) = \frac{n(cGAMP)}{number\ of\ cells} = \frac{0.34\ \mu mol}{0.75 \times 10^{12}} \approx 0.45 \times 10^{-18}\ \text{mol} = 0.45\ \text{attomol}$$

The volume of *E. coli* cell is $10^{-15}$ L. The concentration of 2′,3′-cGAMP in cGAS expressing *E. coli* cells was determined as:

$$[cGAMP\ per\ cell] = \frac{n(cGAMP\ per\ cell)}{cell\ volume} = \frac{0.45 \times 10^{-18}\ mol}{10^{-15}\ L} \approx 0.45 \times 10^{-3}\ \text{M} = 0.45\ \text{mM}$$

**Determination of 2′, 3′-cGAMP concentration in L929 and HEK293T cell extracts**

From the linear regression of the standard curve, shown in Figure 4E, the standard curve fit the equation $Y = mX + C$ gave $1/\text{m} = 1.67 * 10^{-5}\ \mu M$ and $C = 150517 \pm 22135$ with an $R^2$ value of 0.98.

For measuring the average amount of 2′,3′-cGAMP in each dsDNA-stimulated cell, $6 \times 10^6$ DNA-stimulated cells were lysed, extracted and concentrated to give 20 µL cell extract, and 2 µL of the cell extract was added to a solution with final volume of 25 µL for fluorescence measurement. The fluorescence of this solution was measured to be 239874 (figure 4E, average of two independent biological replicates).

Thus, the concentration of 2′,3′-cGAMP in the 25 µL measurement solution was calculated to be:

$$c\ (cGAMP) = \frac{Y - C}{m} = (239874 - 150517) \times (1.67 \times 10^{-5})\ \mu M = 1.5\ \mu M$$

Then, the amount of 2′,3′-cGAMP in the 2 µL cell extract was:

$$n(cGAMP) = c(cGAMP) \times volume = 1.5\ \mu M \times 25\ \mu L = 37\ \text{pmol}$$

Lastly, the amount of 2′,3′-cGAMP per cell was determined as:

$$n(cGAMP\ per\ cell) = \frac{n(cGAMP)}{number\ of\ cells} = \frac{37\ pmol \times 10}{6 \times 10^6} \approx 6 \times 10^{-17}\ \text{mol} = 60\ \text{attomol}$$

$$n(cGAMP\ per\ cell) \approx 6 \times 10^{-17}\ \text{mol} \times \frac{6.022 \times 10^{23}\ molecules}{mol} = 3.6 \times 10^7\ molecules$$

In conclusion, DNA stimulation by transfection resulted in 60 attomoles of 2′, 3′-cGAMP produced on average per L929 cell, or 36 million molecules of 2′, 3′-cGAMP per cell.

Very recently, an LC-MS/MS method has been developed for quantitation of 2′, 3′-cGAMP (Paijo et al., 2016). According to Figure 3 in this research article (Paijo et al., 2016), the amount of 2′, 3′-cGAMP produced upon HCMV virus infection was measured in the range of 1 to 3 fmol/$10^4$ cells.

$$n(cGAMP\ per\ cell) = \frac{n(cGAMP)}{number\ of\ cells} = \frac{1\ fmol}{10^4} = 1 \times 10^{-19}\ \text{mol} = 0.1\ \text{attomol}$$

$$n(cGAMP\ per\ cell) = 1 \times 10^{-19}\ \text{mol} \times \frac{6.022 \times 10^{23}\ molecules}{mol} \approx 6 \times 10^4\ molecules$$

The current lower limit of detection of our fluorescent biosensor is ~1 µM or 40 attomoles per cell. Thus, improving biosensor sensitivity by 133-($\frac{40\ attomoles}{0.3\ attomoles} = 133$ ) to 400-fold ($\frac{40\ attomoles}{0.1\ attomoles} = 400$ ) would provide a high-throughput method to analyze viral-induced 2′, 3′-cGAMP levels.

**Supplemental References**


Folcher, M., Oesterle, S., Zwicky, K., Thekkottil, T., Heymoz, J., Hohmann, M., Christen, M., Daoud El-Baba, M., Buchmann, P., and Fussenegger, M. (2014). Mind-controlled transgene expression by a wireless-powered optogenetic designer cell implant. Nat Commun *5*, 5392.

Hallberg, Z.F., Wang, X.C., Wright, T.A., Nan, B., Ad, O., Yeo, J., and Hammond, M.C. (2016). Hybrid promiscuous (Hypr) GGDEF enzymes produce cyclic AMP-GMP (3', 3'-cGAMP). Proc Natl Acad Sci U S A *113*, 1790-1795.

Kellenberger, C.A., Chen, C., Whiteley, A.T., Portnoy, D.A., and Hammond, M.C. (2015a). RNA-Based Fluorescent Biosensors for Live Cell Imaging of Second Messenger Cyclic di-AMP. J Am Chem Soc *137*, 6432-6435.

Kellenberger, C.A., Hallberg, Z.F., and Hammond, M.C. (2015b). Live Cell Imaging Using Riboswitch-Spinach tRNA Fusions as Metabolite-Sensing Fluorescent Biosensors. Methods Mol Biol *1316*, 87-103.

Kellenberger, C.A., Wilson, S.C., Hickey, S.F., Gonzalez, T.L., Su, Y., Hallberg, Z.F., Brewer, T.F., Iavarone, A.T., Carlson, H.K., Hsieh, Y.F., *et al.* (2015c). GEMM-I riboswitches from Geobacter sense the bacterial second messenger cyclic AMP-GMP. Proc Natl Acad Sci U S A *112*, 5383-5388.

Kellenberger, C.A., Wilson, S.C., Sales-Lee, J., and Hammond, M.C. (2013). RNA-based fluorescent biosensors for live cell imaging of second messengers cyclic di-GMP and cyclic AMP-GMP. J Am Chem Soc *135*, 4906-4909.

Paijo, J., Doring, M., Spanier, J., Grabski, E., Nooruzzaman, M., Schmidt, T., Witte, G., Messerle, M., Hornung, V., Kaever, V., *et al.* (2016). cGAS Senses Human Cytomegalovirus and Induces Type I Interferon Responses in Human Monocyte-Derived Cells. PLoS Pathog *12*, e1005546.

Ponchon, L., and Dardel, F. (2007). Recombinant RNA technology: the tRNA scaffold. Nat Methods *4*, 571-576.

Song, W., Strack, R.L., Svensen, N., and Jaffrey, S.R. (2014). Plug-and-play fluorophores extend the spectral properties of Spinach. J Am Chem Soc *136*, 1198-1201.

Spangler, C., Bohm, A., Jenal, U., Seifert, R., and Kaever, V. (2010). A liquid chromatography-coupled tandem mass spectrometry method for quantitation of cyclic di-guanosine monophosphate. J Microbiol Methods *81*, 226-231.

Su, Y., Hickey, S.F., Keyser, S.G., and Hammond, M.C. (2016). In Vitro and In Vivo Enzyme Activity Screening via RNA-Based Fluorescent Biosensors for S-Adenosyl-l-homocysteine (SAH). J Am Chem Soc *138*, 7040-7047.

Weber, H., Pesavento, C., Possling, A., Tischendorf, G., and Hengge, R. (2006). Cyclic-di-GMP-mediated signalling within the sigma network of Escherichia coli. Mol Microbiol *62*, 1014-1034.